ARTICLE

Received 00th January 20xx,

Accepted 00th January 20xx

DOI: 10.1039/x0xx00000x

2D Boron Nanosheets Architectonics: Opening New Territories by Smart Functionalization

Chao Han[a], Rui Han[a], Xin Zhang[a], Zhimei Xu[a], Weijie Li[b], Yusuke Yamauchi[c,*] and Zhenguo Huang[a,d*]

Due to its low atomic weight, two-dimensional structure, and unique physical and chemical properties, borophene has attracted strong interests from researchers across different fields. Currently, the experimentally realized polymorphs of single-atomic-layered borophene are all grown on substrates and free-standing forms are yet to be obtained, thus restricting the applications. Functionalizing borophene and boron nanosheets, such as attachment of surface functional groups, heteroatom doping, and formation of composites, not only improves structural stability but also generate new physical and chemical properties. Therefore, functionalized borophene/boron nanosheets with new features bears more versatile applications than the pristine ones. This review summarizes the recent advances in both theoretical prediction and experimental work of the functionalized borophene/boron nanosheets. Various functionalization techniques are systematically reviewed with in-depth discussion of their effects on the properties and performance when utilized in various devices. The advantages and limitations of the functionalization methods are discussed with the aim to stimulating thoughts for future research on boron nanosheets, which are believed to possess a plethora of applications in fields such as electronics, energy, biochemistry, optics, just to name a few.

1. Introduction

Two-dimensional (2D) materials such as graphene, transition metal chalcogenides, hexagonal boron nitride possess various potential applications due to their tunable electronic structures, large surface areas, robust mechanical properties, and ease of integrating into devices.[1-9] Although still in its infancy, the research on 2D boron has attracted tremendous interests recently.[10-22] Compared with graphene, transition metal dichalcogenides (TMD) and other 2D materials, 2D boron stands out because of its unique physical and chemical properties. (i) Boron is the lightest metalloid which allows for light-weight nano-devices.[23] (ii) The electron-deficient nature of Boron induces different atomic configurations. As shown in **Figure 1**, four phases (corrugated *2-Pmmn*, flat β_{12}, flat χ_3 and flat graphene-like phases) of borophene have been grown on Ag or Al (111) substrates under ultrahigh vacuum since 2015.[24-27] This offers a vast new platform for electronic structure tuning and extensive potential applications. (iii) Compared with other 2D materials, it has highly delocalized bonds due to electron deficiency.[28] Consequently, B-B bond is neither entirely covalent nor metallic, endowing borophene intriguing electronic, optical, thermal, and chemical properties.[10, 12, 29-35] The bottom-up synthesis of single layer borophene typically requires ultra-high vacuum and the transfer of borophene to another support remains elusive because of its strong interaction with metallic substrates and poor stability under ambient conditions.[13, 14, 27] This poses great difficulty in measuring the intrinsic properties, let alone exploring its applications in devices involving high chemistry dynamics, as shown in **Figure 2**.

On the other hand, free-standing boron nanosheets have been effectively prepared via top-down approaches, mainly by liquid phase exfoliation (LPE) of bulk boron or MgB_2.[36-39] During this process, various functional groups in the liquid media are simultaneously attached to the surface of boron sheets.[37, 39] These functional groups can stablize the exfoliated boron nanosheets and simultaneously tune their properties, therefore leading to versatile applications. Although these free-standing boron nanosheets have been generally termed “borophene”, they do not exhibit the same characteristics as single atomic layered borophene due to the changes in atomic configuation, the increased thickness, and more importantly, the attached functional groups.[12, 15-17, 20, 21] Please note that the term “borophene” mentioned hereinafter represents the single atomic layered elemental boron nanosheets.

Considering the variety of functionalization and consequential applications for the emerging 2D boron nanosheets, it is beneficial to have a concerted discussion on this aspect by reviewing relevant publications (Figure 2), and therefore this

[a] School of Civil and Environmental Engineering, Faculty of Engineering and Information Technology, University of Technology Sydney, NSW 2007, Australia
[b] Institute for Superconducting & Electronic Materials, AIIM Building, Innovation Campus, University of Wollongong, Squires Way, North Wollongong, NSW 2500, Australia
[c] Australian Institute for Bioengineering and Nanotechnology (AIBN) and School of Chemical Engineering, The University of Queensland, Brisbane, QLD 4072, Australia
[d] Centre for Green Technology, Faculty of Engineering and Information Technology, University of Technology Sydney, NSW 2007, Australia

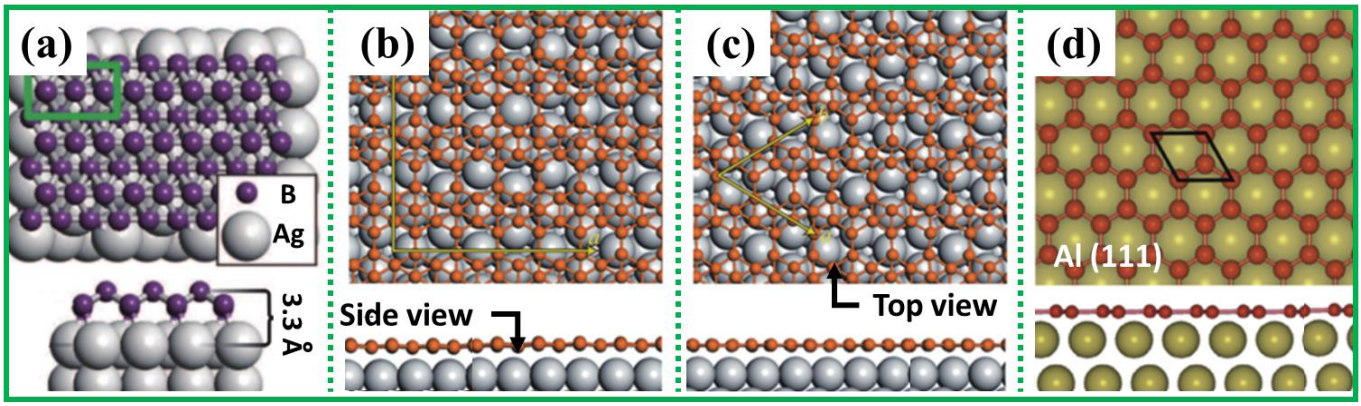

Figure 1. Structure of borophene grown on Ag/Al (111) substrate: (a) *2-Pmmn* borophene; (b) β_{12} borophene (α-borophene); (c) χ_3 borophene; (d) Graphene-like borophene.[24-26] Reproduced with permission. Copyright 2016, Nature Publishing Group; Copyright 2018, Elsevier; Copyright 2015, American Association for the Advancement of Science.

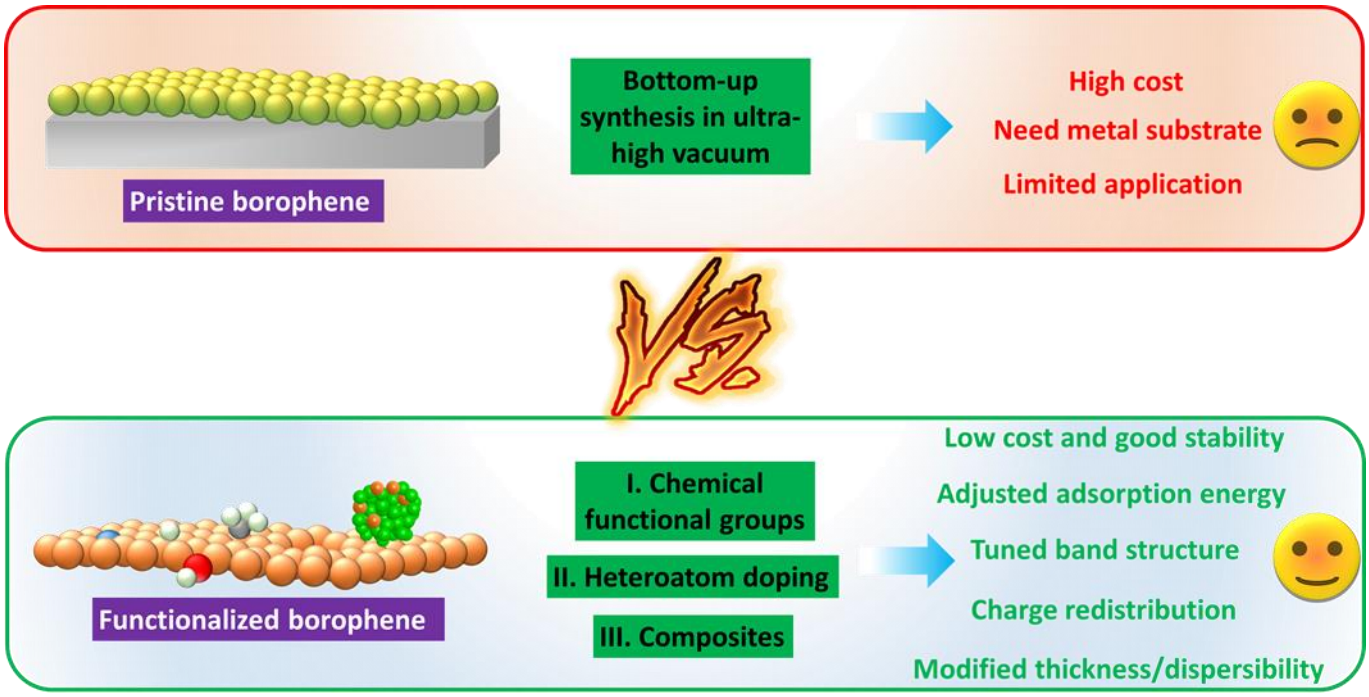

Figure 2. Merits of the functionalized 2D boron nanosheets.

work has different focus than the available reviews.[10-13, 15, 16, 18-20, 22, 28, 30, 40-42]

Herein the term "functionalization" is defined as the introduction of heterostructures that affects the physical and chemical properties of the boron nanosheets. Specifically, the functionalization includes chemical groups, dopants, and strongly interacted composites (Figure 2). Both theoretical predictions and experiments demonstrating the efficacy of functionalization on property modulations are summarized. We hope this work would shed light on how to tune the properties of 2D boron via functionalization, which helps to explore its applications.

2. Chemical functional groups

Chemical functionalization tailors the properties of borophene through the attachment/integration of different chemical entities, such as atoms or functional groups, onto its planar surfaces. These attachments cause electron redistribution, adjusted adsorption energy towards different species and tuned band structures. The strong interactions between boron and the attachments also alter the wettability, thickness and dispersibility of boron nanosheets in various solvents, which will further broaden its applications (Figure 2). Generally, there are three effective routes to introduce functionalization: (i) top-down synthesis of boron nanosheets using a liquid/gas phase exfoliation method; (ii) bottom-up chemical vapor deposition or molecular beam epitaxy in certain atmosphere; and (iii) ligand exchange after obtaining boron nanosheets.[15, 43-46]

2.1 Hydrogenated boron nanosheets

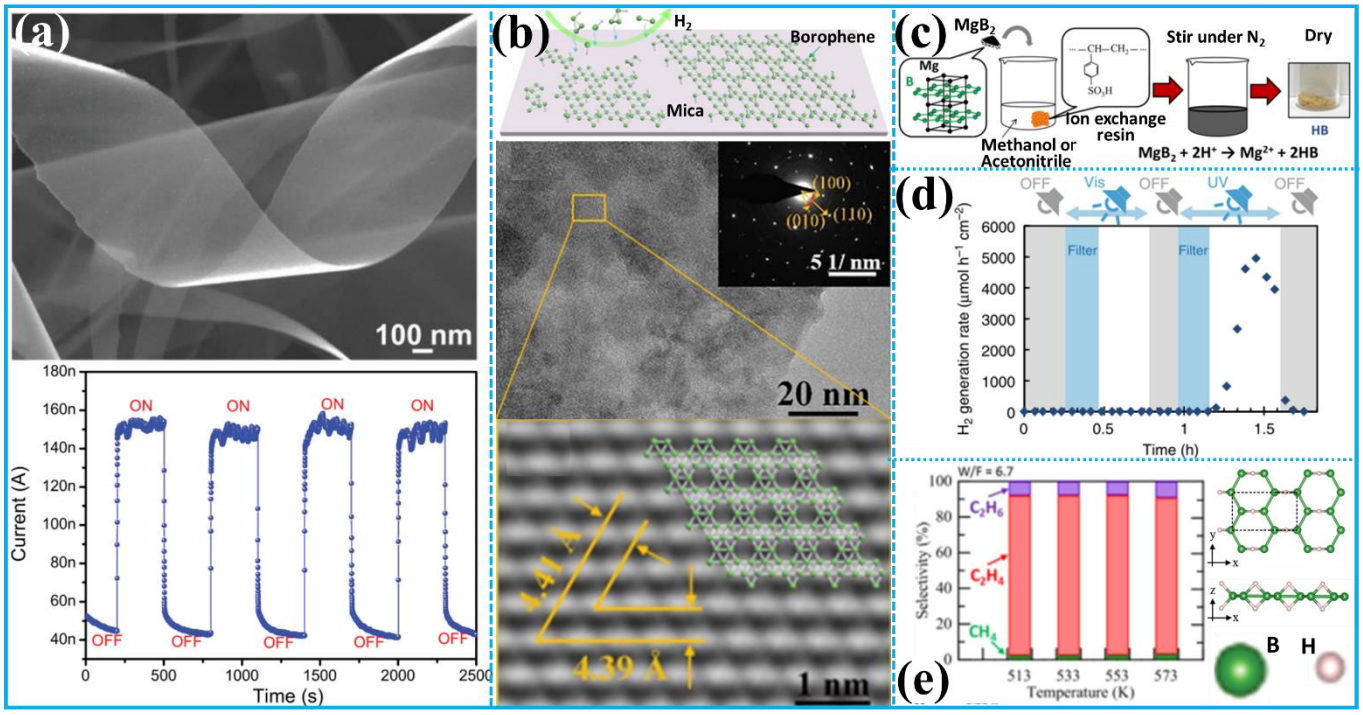

Figure 3. Synthesis, characterization and application of HB nanosheets. (a) Boron nanosheets prepared by thermal decomposition of B_2H_6 (upper) and its photo-response under 325 nm light (lower). Reproduced with permission from Ref.[47] Copyright 2015, Wiley-VCH GmbH. (b) The HB nanosheets grown on mica substrate prepared by chemical vapor deposition from B and B_2O_3 powders in H_2 atmosphere. Reproduced with permission from Ref.[48] Copyright 2021, American Chemical Society. (c) Schematic illustration of preparation of HB nanosheets by a cation exchange process. Reproduced with permission from Ref.[49] Copyright 2017, American Chemical Society. (d) H_2 release from HB under light. Reproduced with permission from Ref.[50] Copyright 2019, Springer Nature. (e) The selectivity of HB nanosheets in ethanol reforming reaction. Reproduced with permission from Ref.[51] Copyright 2019, American Chemical Society.

Hydrogen atom is the simplest chemical functional group that can stabilize borophene forming hydrogen boride (HB), which is stable in air or water.[10, 52-54] The improved stability after hydronation is due to electron transfer induced bonding re-arrangement.[55] The zero band gap of pristine borophene is also opened due to hydrogenation and the Fermi velocity of HB reaches 3.5×10^6 m/s, which is higher than graphene.[55, 56] This means that HB is a small band gap semiconductor, the electrons of which can be easily excited. The formation of B-H-B bridging bond also modulate the mechanical properties.[53, 55, 57] HB nanosheets was realized experimentally in three ways: (i) decomposition of borane in H_2;[58] (ii) chemical vapor deposition from solid powders (B, B_2O_3, or $NaBH_4$) in H_2;[44, 48, 59] and (iii) cation exchange reaction with organic solvents/cation exchange resins that can provide protons.[49, 51, 60, 61] For example, Xu *et al.* prepared HB nanosheets on a silicon wafer via chemical vapor deposition using borane gas (5% B_2H_6 + 95% Ar) and the nanosheets show excellent photo-excitation behavior because of the slightly opened band gap, as illustrated in **Figure 3**(a).[47] Tai *et al.* synthesized HB nanosheets via a thermal decomposition of $NaBH_4$ in H_2/Ar atmosphere [Figure 3(b)].[44, 48] As demonstrated in Figure 3(c), Kondo *et al.* obtained HB nanosheets from MgB_2 powders by a cation exchange method in acetonitrile using a cation exchange resin.[49, 60]

HB nanosheets can be a high-performance hydrogen carrier [Figure 3(d)][50, 62]. Miyauchi *et al.* found that a large amount of gaseous H_2 (8 wt.%) was released from HB nanosheets under photoirradiation. Both the experimental and theoretical investigations suggest that H_2 release is driven by the excited electrons in the antibonding state of the H orbital, leading to the self-reduction of protons and the generation of H_2.[50] HB nanosheets serve as a mild reducing agent and a catalyst towards ethanol reforming reaction [Figure 3(e)] [51, 61, 63]. According to Kondo's work, the redox potential of the HB sheets is between -0.277 and -0.257 V versus standard hydrogen electrode (SHE).[63] The reduction property of HB nanosheets is related to H functionalization. Hydrogen in HB are protic (H^+) rather than hydridic (H^-), based on the B 1s core-level states and the Hammett acidity function (H_0 or acid strength between 0.43-1.50).[49, 51, 63] This explains the reduction of metal ions such as Cu^{2+} by the negatively charged boron in HB to their neutral state facilitated by an exchange between metal ions and H^+ of HB.[63] Benefiting from the protonic character of H^+ in HB, the HB nanosheets can also be applied as a catalyst in certain proton related reactions, such as ethanol reforming reaction ($\boldsymbol{C_2H_5OH \rightarrow C_2H_4 + H_2O}$).[51, 61] This conversion is driven by dehydration where the -OH in ethanol combines with proton from the HB sheet, resulting in the formation of C_2H_5-B and H_2O. C_2H_5-B was then transformed to C_2H_4 and HB. Besides these experimental works, HB is also predicted to be an ideal light-weight anode for potassium ion batteries due to excellent mechanical properties, low voltage of ~0.24 V (*vs*. K/K^+), as well as desired K-ion affinity and hopping resistance. H vacancies in

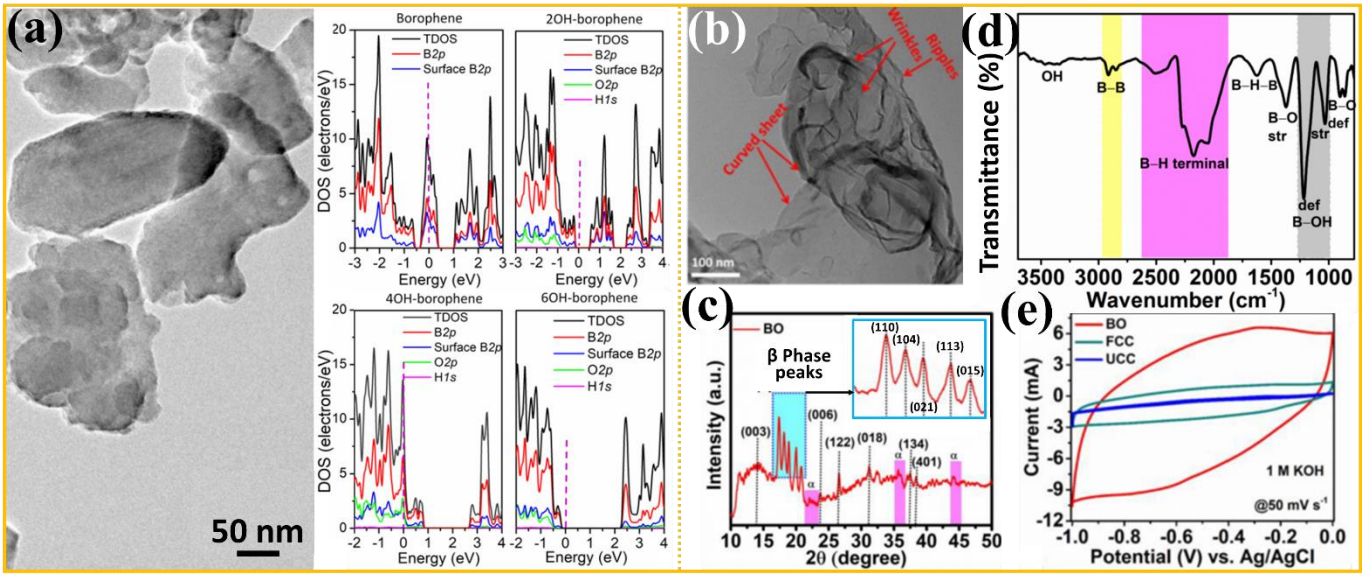

Figure 4. Morphological and structural information of B-OH nanosheets and performance in supercapacitor applications. (a) TEM image of the B-OH nanosheets prepared by liquid phase exfoliation (LPE); the DOS for bilayer borophene and bilayer borophene coordinated with 2OH, 4OH, and 6OH groups, respectively. The dotted line represents the Fermi level. Reproduced with permission from Ref. [37] Copyright 2020, Wiley-VCH GmbH. For B-OH nanosheets prepared by Hummer's method, (b)-(e) TEM image, XRD pattern, FT-IR spectrum and supercapacitor performance in 1 M KOH electrolyte. BO, UCC and FCC represent B-OH nanosheet, blank carbon cloth and functionalized carbon cloth, respectively. Reproduced with permission from Ref.[39] Copyright 2021, Elsevier.

HB nanosheets were found to improve both the K-ion intercalation and K-ion hopping, yielding a high theoretical capacity (1138 mAh/g).[64]

In all, owing to the functionalization by the simplest and smallest H atoms, borophene is stabilized via electron redistribution with little deterioration in its conductivity. Hydrogenation also endows potential applications of HB in photodetector, electronics, hydrogen carrier, reduction reaction, and catalysis.

2.2 Oxidized boron nanosheets

Due to high reactivity, partial oxidation of borophene takes place within several hours under ambient conditions.[26] Because of the high electronegativity of oxygen (3.44 for O and 2.04 for B, Pauling scale), B atoms in borophene bound to O atom are displaced slightly out of the top layer and move closer to each other, inducing a series of structural and property fluctuations. According to theoretical prediction, new states can be introduced into the density of states of pristine borophene by the B-O *p* orbital hybridization and the resultant structure rearrangement.[65] He *et al*. found that a large amount of electrons were transferred from electron-deficient borophene layer to electrophilic O atoms, transforming metallic borophene into p-type semiconductor in the oxidation process.[66] Depending on the degree of oxidation, the mechanical and electronic structure of boron nanosheets could be adjusted to different extent.[66-70]

The oxygen functionalization can be achieved by oxidizing borophene or borides in dry air. Yamamoto's group synthesized oxidized boron nanosheets ($B_{4.27}KO_3$) analogue via oxidation of KBH_4; in which layers of boron-oxygen networks and potassium cations were positioned in an alternating manner.[71] $B_{4.27}KO_3$ demonstrated an anisotropic conductivity due to its unique layered structure. Chahal *et al*. investigated the properties of BO_x nanosheets prepared via micromechanical exfoliation.[72] They found the Raman signals of methylene blue on the oxidized boron nanosheets were significantly enhanced compared with those on bare gold. It is believed that oxygen functionalization causes charge transfer between B and O, which leads to frequency coincidence (or resonance) with the incident photon energy and greatly enhances the Raman scattering intensity.[73] Moultos *et al*. simulated the suitability of Li, Na, and K decorations on 2D honeycomb borophene oxide (B_2O) for H_2 storage.[74] They found that B_2O has lower formation energy compared with other 2D B_xO. A high theoretical gravimetric density of 8.3 wt % H could be achieved for the Li-decorated B_2O structure due to suitable adsorption energy towards H_2. Upon oxidation, new density of states of O appears near the Fermi level of pristine borophene, while the electron effective masses increase and velocities decrease. Therefore, with appropriate degree of oxidation, borophene could display a large increase in visible light adsorption and reflectance in the infrared region, making it suitable for transparent conductive material.[65, 75] Yan *et al*. predicted the existence of superconductivity in honeycomb borophene oxide (B_2O). A superconducting transition temperature (T_c) of ~10.3 K could be reached, higher than many 2D borides (0.2-7.8 K).[70] The superconductivity mainly originates from the out-of-plane soft-mode vibrations of the system, which are significantly enhanced by oxygen functionalization.

Due to the electron deficiency of B and high electronegativity of O, it is difficult to precisely control the degree of oxidation in borophene. This has been experimentally verified by Chahal's work, where various oxides such as BO, B_2O, B_4O, B_5O, B_7O and B_8O were found when boron nanosheet was thermally oxidized.[72] To achieve the desired results for the right applicati-

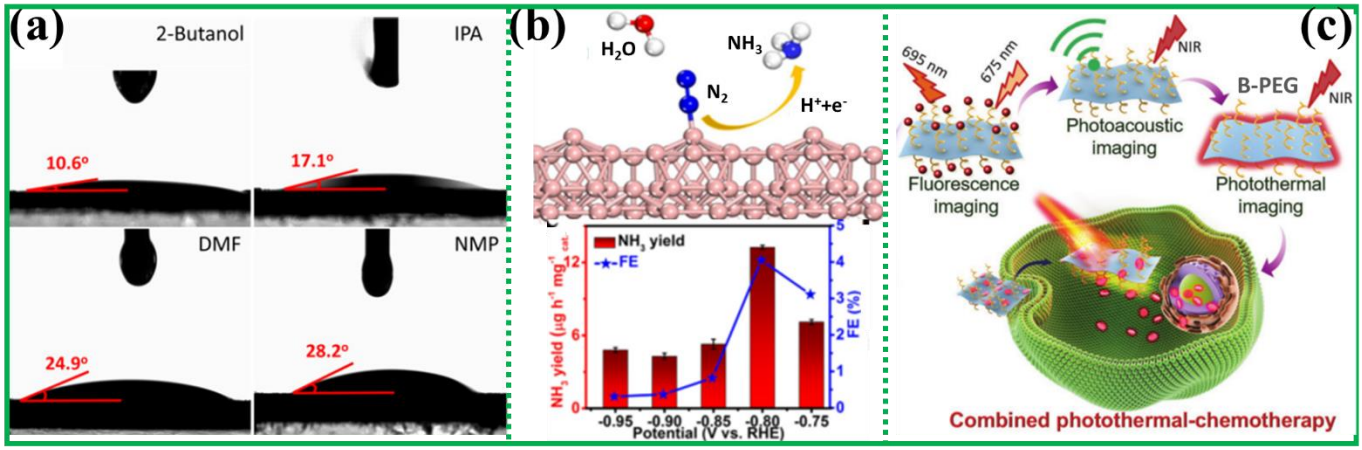

Figure 5. Effect of different solvents on chemical functionalization. (a) Contact angles between water and boron nanosheets exfoliated in 2-butanol, IPA, DMF, and NMP, respectively. Reproduced with permission from Ref.[37] Copyright 2020, Wiley-VCH GmbH. (b) Schematic illustration and catalytic performance of nitrogen reduction reaction catalyzed by boron nanosheets exfoliated in IPA. Reproduced with permission from Ref.[21] Copyright 2019, American Chemical Society. (c) Schematics showing the PEG functionalized boron nanosheets as a photonic nanomedicine for multimodal imaging-guided cancer therapy. Reproduced with permission from Ref.[76] Copyright 2018, Wiley-VCH GmbH.

-ons, methods with better controllability are needed to control the oxidation. From a different perspective, the great combination of oxides would enable great tunability leading to a plethora of applications.

2.3 Hydroxylated boron nanosheets

Hydroxylation is not only an important technique to endow boron nanosheets and borophene with intriguing properties and applications in various fields, but also serves as the initiators for further reactions with other complex functional groups.[77] The OH functionalization can be simply achieved by immersing or fabricating the boron nanosheets within aqueous solutions.[43, 78-81]

In 2017, Kondo *et al*. prepared hydroxyl-functionalized boron nanosheets (B-OH) by an ion exchange reaction in water.[80] The ion-exchange reaction between protons in water and part of the Mg cations was followed by a hydrolysis reaction between the HB and water, producing H_2 and Mg-deficient hydroxyl-functionalized boron sheets. Apart from MgB_2, elemental boron also reacts with water to form hydroxylated boron nanosheets.[82] James *et al*. prepared B-OH nanosheets using this method and found that the B-OH nanosheets exhibited a standard reduction potential around 0.16 V (versus SHE) in neutral aqueous medium and reduced quinone-based molecules, $KMnO_4$, graphene oxide and gold ions.[79] Wang *et al*. synthesized B-OH nanosheets by a two-step liquid-phase exfoliation method.[37] In their work, boron powders were firstly exfoliated by probe sonication in 2-butanol, and hydroxylation was then carried out by ice-bath sonication in aqueous KOH. The B-OH nanosheets also feature better stability and dispersibility in aqueous solutions, making it more suitable as reactive templates onto which another nano system could be integrated via *in situ* reduction.

As demonstrated in **Figure 4**(a), the OH group can open up and tune the band gap of pristine borophene due to the hybridization of oxygen *p* orbital with boron *p* orbit. The theoretically predicted band gaps ranged from 1.41 eV for bulk B to 1.98 eV for 4OH-coordinated borophene and to 2.55 eV for 6OH-coordinated borophene [Figure 4(a)].[37] The tunable band gap endows the B-OH nanosheets a promising application as a high-performance photo detector.[37] Joshi *et al*. synthesized B-OH nanosheets [Figure 4(b)] using the Hummer's method and applied it as an electrode in supercapacitors.[39] Although the product was dubbed "borophene oxide", the boron nanosheets was actually covered by both -OH and -O groups. Their results showed that hydroxylation is effective in achieving a higher capacitive performance as the -OH groups act as active sites for ion adsorption/desorption.[39] Using a similar approach, Ranjan *et al*. found the specific capacity of the supercapacitor reached 4941 mAh g^{-1}, exceeding those of existing 2D materials and their hybrids.[17] Zhang *et al*. obtained hydroxylated boron nanosheets via direct exfoliation of boron powders in water, and the product showed good terahertz microwave shielding performance.[83] Besides the good conductivity of boron nanosheets, it was postulated that -OH groups also contributed to microwave shielding by creating out of plane vibration.

As a hydrophilic functional group, hydroxyl functionalization renders the boron nanosheets good solubility and dispersibility in aqueous solutions, making it ready for more applications than pristine borophene. More importantly, hydroxylation process is more controllable than oxidation, and it can be realized more effectively than hydrogenation.

2.4 Solvent-derived functional groups

Liquid phase exfoliation (LPE) has been widely used to generate boron nanosheets.[18] The choice of solvents has significant impact on the yield, thickness and dispersibility of boron nanosheets due to different sizes, viscosity, polarity and compositions of the solvents [**Figure 5**(a)].[84-86] This means boron nanosheets exfoliated in different solvents could show different properties. The functional groups introduced by different organic solvents, such as alcohol, amide, dimethylformamide (DMF), N-Methyl-2-pyrrolidone (NMP), dimethyl sulfoxide (DMSO), usually exhibit a combination of -O,

-OH, -NH_2, -S=O, alkyl, alkoxy groups, etc., which can lead to broad applications but at the same time give rise to difficulty in understanding the individual effect of each functional group.

Alcohols are efficient solvents that aid to producing boron nanosheets in high yield.[84] Alcohols can tune the band gap of boron nanosheets and borophene due to -OH and -H groups, and the resultant boron nanosheets have been tested for catalysts and optical devices.[21, 87] Sun *et al*. prepared boron nanosheets in isopropanol (IPA) and found that the prepared boron nanosheets can effectively catalyze nitrogen reduction reaction (NRR) with a high Faradaic efficiency of 4.04 % and a high NH_3 yield of 13.22 $\mu g.h^{-1}.mg_{cat}^{-1}$ at -0.80 V.[21] The active sites were determined to be the oxidized and H-deactivated B atoms [Figure 5(b)]. Moreover, alcohols can also introduce carbonyl, alkyl and alkoxyl (-O-R) groups, which can increase the stability of boron nanosheets in complex organics. The -OH group introduced by the alcohols increases the dispersibility of boron nanosheets in aqueous systems. These all endow alcohol functionalized boron nanosheets with desired properties for bio-applications. One example was reported by Ma *et al*., who prepared boron nanosheets in IPA with an average thickness of 1.5 nm. The ultrathin B-IPA nanosheets were functionalized with -OH, -H, -C=O and -O groups and exhibited strong blue fluorescence, making it a low-toxic bio-imaging agent.[36] Boron nanosheets obtained in ethylene glycol (EG) and polyethylene glycol (PEG) were employed as radiosensitizer in boron neutron capture therapy (BNCT), photothermal therapy (PTT) and particle therapy (PT) owing to their excellent photothermal effect, tunable bandgap, and good biocompatibility [Figure 5(c)].[45, 76, 88] The successful surface functionalization by PEG group and LPE method was identified by Fourier-transform infrared spectroscopy (FT-IR) analysis.[76] The amounts of PEG group have significant effects on its photo-thermal efficiency.[76] This is reasonable since different amounts of functionalization leads to boron nanosheets with different sizes and defects. Zhou *et al*. introduced methyl group (-CH_3) by exfoliating MgB_2 in methanol with the help of iodine and applied the product as an anode in lithium ion batteries (LIB).[89] This methyl functionalized boron nanosheets, which is evidenced by FT-IR analysis, showed enhanced environmental stability. They also found that the boron electrode reacted with nucleophilic organics (such as $(CH_2OCO_2Li)_2$) present in the solid electrolyte interface (SEI) forming a passivation layer, which retarded the diffusion of Li^+ ions. Thus the boron nanosheet anode performance in LIBs can be modulated via varying the surface functional groups.[89]

Different from alcohols, DMF contains -CHO and -$N(CH_3)_2$ groups, which may lead to different properties. Comparing with boron nanosheets prepared in IPA, the sheets prepared in DMF dispersed better (up to 1.16 mg/mL) and were more stable under ambient conditions. The functionalization of boron nanosheets was confirmed by C-N and C-B bonds observed in the X-ray photoelectron spectra.[85] The DMF-exfoliated few-layer B sheets were applied as supercapacitor electrode materials. Employing ionic liquid (1-butyl-3-methylimidazolium hexafluorophosphate) as the electrolyte, the supercapacitor possessed a potential window as large as 3.0 V and exhibited a maximum specific capacitance of 142.6 F/g at a current density of 0.3 A/g.[85] This result is comparable to -OH functionalized boron nanosheets (3.0 V potential window, capacitance of 78.88 F/g at 2 A/g).[39] This excellent performance was attributed to the DMF functionalization. For one thing, the well dispersed boron nanosheet in DMF offers high surface area and more active sites; for another, the DMF coating endows the sample good wettability towards the ionic liquid, leading to low contact resistance.[85] Tao *et al*. prepared boron nanosheets in DMSO with the product displaying strong signals of C-S, B-S, -CH_3 in FT-IR spectrum.[90] When used as a LIB anode, the B-S bond was believed to stabilize the boron nanosheets and increased the adsorption energy towards Li^+.

LPE preparation of boron nanosheets in different solvents can indeed introduce different functional groups onto the boron nanosheets. These functional groups can affect the sample properties in two ways, both of which in turn have profound effects on their applications. First, the yield, thickness, solubility and stability could be effectively adjusted by these functional groups.[38, 91] Second, functional groups can alter the adsorption energy towards different species in the reaction, and therefore change the reaction kinetics.[90] Note different functional groups could be introduced simultaneously using one single solvent, which consequently bring about multiple variables impacting on the properties. These functional groups could play a synergistic or a competing role in modulating physical and chemical properties. Therefore, in order to optimize certain properties, in-depth studies should be carried out on understanding the effects of individual and a combination of functional groups. This can be achieved when more advanced theoretical and experimental techniques with ever-increasing accuracy at atomic scale are becoming available.

3. Heteroatom doping

Heteroatom doping is another effective strategy to tune the electronic structure of 2D structures.[4, 92, 93] Herein doping refers to the atomic replacement of B by heteroatoms within a boron nanosheet's in-plane structure without forming large domains of the doping atoms. Both metal and non-metal atoms have been explored theoretically, as the dopants.

It has been calculated that most of transition metal doped boron nanosheets can be excellent electrocatalysts towards different reactions because of the tunable electronic structure and suitable adsorption energy towards different intermediates. Generally, the *d* band of these transition metals can hybrid with *p* orbital of boron, leading to tuned bonding and anti-bonding orbital of the B-X (X represents the adsorbed intermediates), which finally adjusts the adsorption energy of the doped boron nanosheets.[94] Water electrolysis, the most promising way to generate green hydrogen, consists of hydrogen evolution reaction (HER) and oxygen evolution reaction (OER). As presented in **Figure 6**(a), it was found that most of the metal (Li, Ti, Sc, V, Fe, Mn, Co, Ni, Ag, Cu, Pt, Pd, Rh, Ir, Ru) doped borophene are good HER catalysts with close to zero hydrogen adsorption energy. Ni and Ti doped borophene are the most promising catalysts for both OER and HER. Noble metal dopants are more beneficial than transition metals for HER and OER because of the optimized adsorption energy towards H and OH.[95-98] While Fe is the most promising dopants for oxygen reduction reaction (ORR) among all the transition metals [Figure 6(b)],[99, 100] Mo and Mn were predicted to be the most efficient borophene dopants towards NRR, since they can

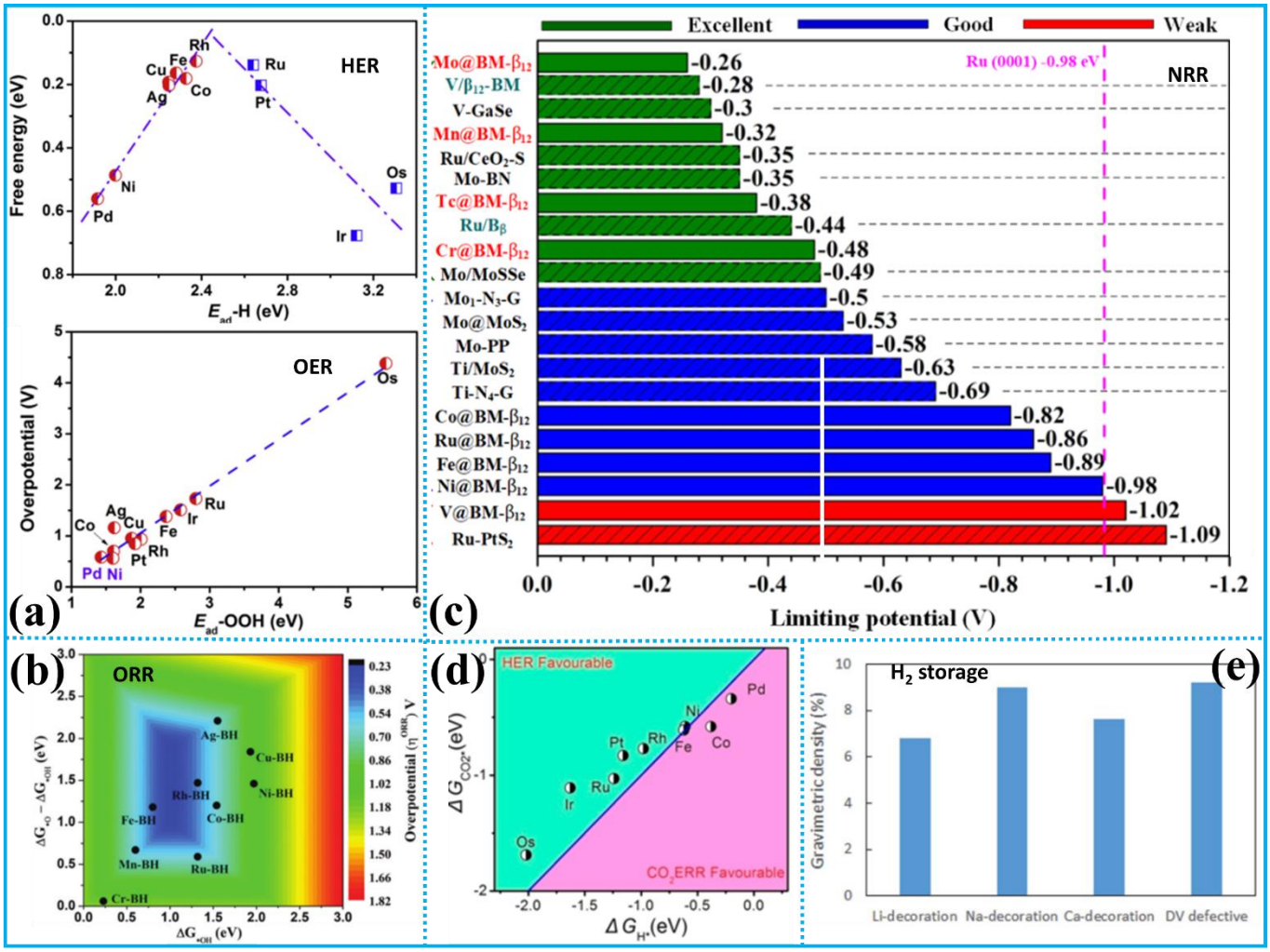

Figure 6. Heteroatom doped borophene and its applications. (a) The HER and OER performance of the α-borophene doped by different metals. The top is the volcano relationship between the E_{ad} of H and the free energy of the rate-determining step of the HER, and the bottom is the relationship between the overpotential of the OER and the E_{ad} of OOH on metal-doped α-borophene. Reproduced with permission from Ref.[97] Copyright 2020, Elsevier. (b) Coloured counter plots of the ORR activity for metal doped HB nanosheets showing the thermodynamic overpotentials η_{ORR} as a function of Gibbs binding free energies of the reaction intermediates. Reproduced with permission from Ref.[99] Copyright 2018, Royal Society of Chemistry. (c) The limiting potentials of NRR for various metal doped borophene. Reproduced with permission from Ref.[101] Copyright 2021, American Chemical Society. (d) Free energies for H and CO_2 adsorption on metal-doped borophenes, which indicates the catalytic activity towards HER and CO2RR, respectively. This indicates that Pd and Co doped borophene are more suitable for CO2RR. Reproduced with permission from Ref.[102] Copyright 2020, American Chemical Society. (e) The hydrogen gravimetric densities for Li, Na and Ca decorated and defective borophene, respectively. Reproduced with permission from Ref.[103] Copyright 2018, Royal Society of Chemistry.

strongly suppress the HER side reactions to improve the NRR selectivity [Figure 6(c)].[101, 104, 105] Xu *et al*. studied the catalytic activity of metal doped borophene towards CO_2 reduction reaction (CO2RR).[102] The results showed that CO2RR was energetically more favorable than HER on Co- and Pd-doped α-borophene nanosheets because of moderate adsorption energy. The theoretical works proved that the electrocatalytic activity of these heteroatom doped borophene is comparable with transition metal-based catalysts.[106-108]

Certain metal doped borophene has stronger affinity towards certain gas molecules than the pristine one, making them suitable for potential applications as gas sensors or adsorbents. For example, Na decorated borophene is suitable for CO adsorption.[109] Kumar's results predicted that the gas adsorbing energy of pristine borophene follows the order of $NO>NO_2>CO>H_2S>NH_3>CO_2$ due to the decreased charge transfer to borophene. Based on this theory, the gas adsorption ability of borophene towards CO_2, CO, NO_2 and NO could be enhanced by V, Ni/Co, Sc/Ti/V/Cr, and Fe/Co doping, respectively.[110] Li, Na, Ca and Ti doped boron nanosheets are suitable for hydrogen storage because of the enhanced hydrogen adsorption energy.[74, 103, 111-114] With an atomic ratio of 1:4 with B, transition metals such as Cr, Mn, Fe, V doping could

induce room temperature ferromagnetism.[115, 116] Al and Ga doping could significantly tune the band gap and optical behavior of borophene due to the *p* orbitals hybridization between B-Al and B-Ga.[117]

For the nonmetal dopant, P and halogens doped borophene have been predicted to have stable structures and can be excellent anode materials in alkali metal ion batteries.[118-122] For example, P-doped borophene nanosheets possess high binding energy of 3.42 eV towards Li. Theoretically, the P doped borophene can adsorb 18 Li^+ to form $Li_{18}B_{23}P$ and exhibit a high capacity up to 1732 mAh/g, higher than that of the pristine phosphorene and pure borophene.[119]

In general, heteroatom doping modifies the electronic structure and adsorption energy towards different intermediates, endowing borophene with new properties such as suitable catalytic activity towards different reactions, optimized adsorption energy towards different gases, and enhanced Li^+/Na^+ ion storage properties. Doping usually introduces corrugation in the basal plane while imparting structural stability to borophene. [117, 121] Up to now, most of the research on heteroatom doping has been theoretical simulations. Experimental evidence is absent because of the difficulty in achieving doping configurations adopted in theoretical studies. More importantly, borophene possesses a high reactivity towards both metal and non-metal elements and borides (such as Fe_xB, BN, BP, etc.) can form when dopants are introduced. The resulting products often contain thermodynamically stable boride domains, i.e., phase separation, rather than structures with doping occurred at specific sites. Limiting doping to atomic level would be highly challenging in a typical laboratory.

4. Composites featuring strong chemical interactions

Integration of another compound with boron nanosheets into heterostructures via strong chemical interactions can display the properties of both B and the hetero-components, and yield an interface with new functionalities, leading to new applications. The interfaces feature interactions in the forms of columbic interactions, or covalent, or ionic bonding.

For nanoparticles and one-dimensional nanostructures, the boron nanosheets act as a support and modulate the composite properties via strong bonding. Tai *et al*. prepared a core-shell structured boron nanosheet-Fe_3O_4 composite via an *in situ* decomposition of $NaBH_4$-Fe_3O_4 mixture in H_2.[123] Strong B-O and B-Fe interactions were evidenced by XPS and FTIR analysis. The boron-functionalized magnetic core-shell nanoparticles had a higher energy level, which increased the number of passing electrons through the Schottky barrier. A nonvolatile rewritable memory device based on this core-shell nanostructures was fabricated, which showed an improved on/off current ratio of 8.23×10^5 (4×10^5 for bare Fe_3O_4) and a lower reset operating voltage of around 0.19 V (1 V for bare Fe_3O_4) as well as good stability. A composite made of rhodium (Rh) nanoparticles (3 nm in size) and conductive boron nanosheets was reported by Chen *et al*.[124] The composite was tested as HER catalyst in both 0.5 M H_2SO_4 and 1 M KOH electrolyte, with an overpotential of only 66 mV and 101 mV to reach the current density of 10 mA cm^{-2}, respectively [**Figure 7**(a)]. Meanwhile, the composite exhibited impressive electrochemical durability in acidic and alkaline media, as well as simulated seawater environment. The strong metal-support interaction (SMSI) between B and Rh, which was evidenced by XPS, was believed to lead to the stability and high conductance of the composite, giving catalyst outstanding HER performance. Karakus *et al.* reported boron nanosheets@polyaniline (PANI) composite for glucose detection. The boron nanosheets prepared via LPE in DMF was negatively charged (evidenced by negative Zeta potential) and thus strongly interacted with the positively charged PANI nanofiber, yielding a higher conductivity in the composite than pristine PANI. The room temperature glucose detection sensitivity of composite nanofiber was increased and the stability was also improved.[125]

Composites of vertically stacked 2D heterostructures could inherit their high surface areas, therefore exhibiting broad applications. Kong *et al*. fabricated the "borophene-graphene" composite by hydrothermal treatment of graphene and boron nanosheets.[126] The composite featured strong C-O-B interactions (evidenced by XPS and FT-IR spectra) and exhibited excellent microwave absorption ability, which was assigned to the improved electron transfer between layers [Figure 7(b)]. Tai *et al*. fabricated "borophene-graphene" composites by heating a mixture of $NaBH_4$ and graphene.[127] The strong interaction between graphene and the boron nanosheets was evidenced by a shift in the binding energy of B element in the XPS spectra compared with single boron nanosheets. Owing to the strong B-C interaction and the sensitivity of 2D boron to water, the composite was assembled into a stable and highly sensitive humidity sensor. Wu and Long *et al.* prepared the boron nanosheets@carbon nanosheets composite, in which B-C bond was confirmed by XPS analysis.[128, 129] The B-C bond not only endows the composite better charge transfer in three dimensions, but also stabilizes the boron nanosheets. The composite was identified as a good electrode material in high performance supercapacitor.[128, 129]

Borophene-MoS_2 nanosheet is another extensively investigated composite. Shen *et al*. theoretically designed a borophene/MoS_2 heterostructure and investigated the adsorption behaviors towards small gas molecules (CO, CO_2, NO, NO_2 and NH_3) on borophene surface.[130] The MoS_2 serves as a substrate to stabilize the borophene and modify its electronic structure to tune the gas adsorption performance. The results indicated that the CO/NO/NO_2/NH_3 molecules can be adsorbed onto the composite by B-C/N bond. Hou *et al*. experimentally demonstrated a boron nanosheet/MoS_2 heterostructure humidity sensor with ultrahigh sensitivity, fast response, long life, and good flexibility.[131] Compared with pristine MoS_2, the XPS peaks of Mo and S in the composite both shifted towards higher binding energy confirming the interaction between MoS_2 and boron nanosheets. These interactions facilitate electron and hole transfer between them because boron nanosheet is a *p*-type semiconductor while MoS_2 is an *n*-type semiconductor. Yin *et al*. loaded boron nanosheets/MoS_2 composite onto a porous substrate for water evaporation and purification.[132] The surface of boron nanosheets contains -OH and -O functional groups, which provide active sites for the deposition of MoS_2 in the synthesis. MoS_2 nanoflowers were successfully grown on boron nanosheet featuring O-S bonding, as evidenced by XPS.

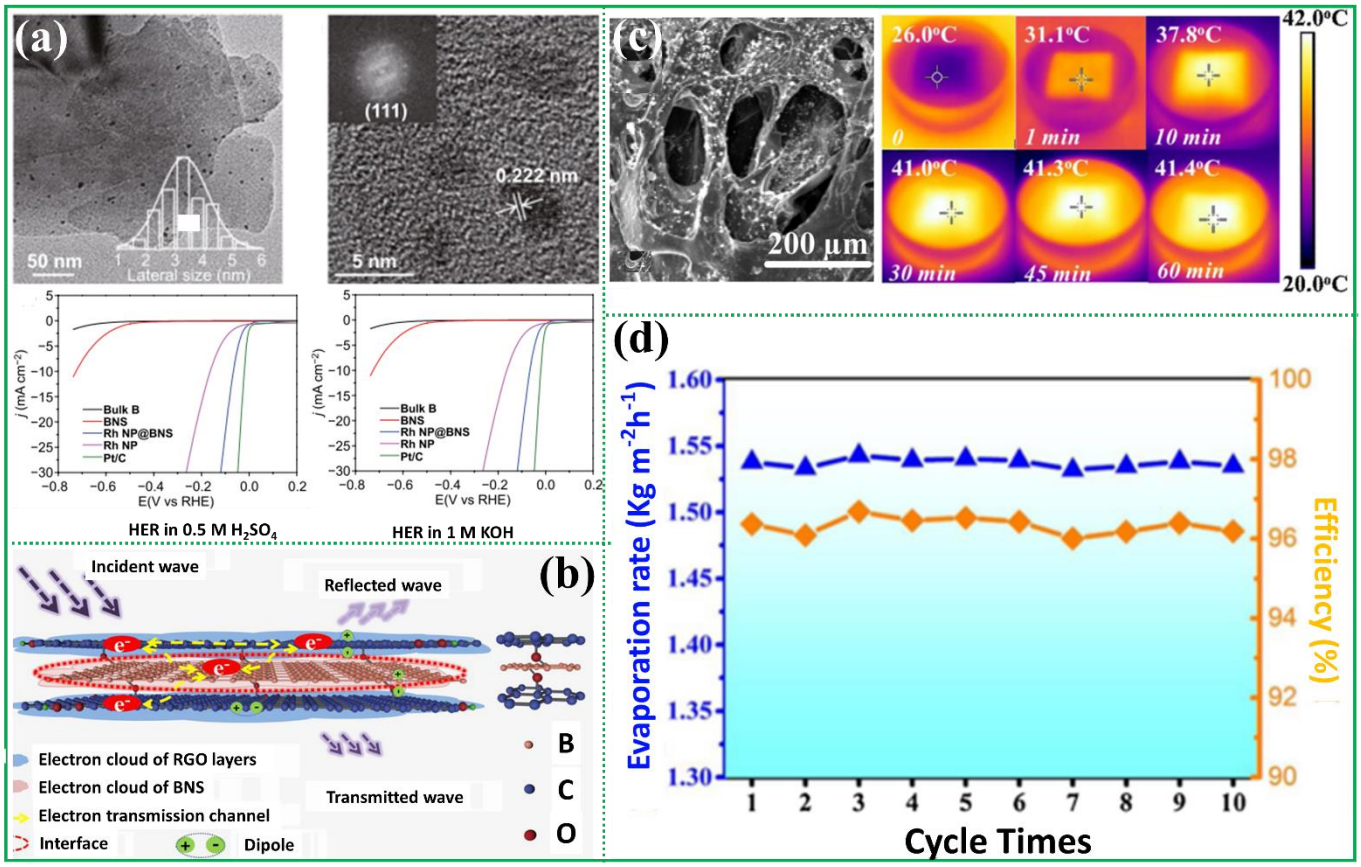

Figure 7. Effect of compositing on boron nanosheets. (a) SEM and TEM images (top) and HER performance (bottom) of the boron nanosheet-Rh composite. Reproduced with permission from Ref.[124] Copyright 2021, Springer Nature. (b) Schematic illustration of the Reproduced with permission from Ref.[126] Copyright 2020, Elsevier. (c) SEM images (left) and the infrared image of the temperature of KBMS (right) over time. KBMS represents the boron nanosheet/MoS_2 loaded porous structure; (d) The evaporation rate and corresponding solar thermal conversion efficiency of KBMS. Reproduced with permission from Ref.[132] Copyright 2021, Elsevier.

The three-dimensional flower-like MoS_2 coated on the boron nanosheets increases the scattering and absorption path of light, which increases the light absorption. The narrow energy band gap and the excellent photothermal conversion effect led to a rapid water evaporation rate (1.538 kg m^{-2} h^{-1}) and high solar evaporation efficiency (96.5 %) under 1 sun radiation (1 kW m^{-2}) [Figure 7(c-d)]. Borophene and blue phosphorene were theoretically predicted to form a P-B-P sandwich composite via B-P bond. The B-P interaction endows the composite with moderate adsorption energy and diffusion barrier towards polysulfides, leading to high capacity and rapid charge/discharge of Li-S batteries.[133] B-P bond was also reported to improve the affinity of blue phosphorene/borophene towards Li^+ ions.[134]

The composite functionalizes borophene via chemical bonding or electrostatic force. The functionalization stabilizes 2D boron, forms an interface with tunable adsorption energy towards different species, and improve the overall conductivity. The composite structure can reap the benefits from both worlds, i.e., the intrinsic versatility of boron nanosheets and the functionalities of the substrate, and the newly emerged interfaces featuring new properties. The sheer number of combinations of boron nanosheets with other 2D materials and nanoparticles enables large room to explore various applications.

5. Summary and outlooks

Boron nanosheets and borophene are fascinating materials since they can adopt various structures and displays unique physical and chemical properties. Generally, preparation of borophene could be classified as top-down and bottom-up routes. The bottom-up route refers to growing borophene on metal substrates under ultra-high vacuum conditions, such as chemical vapor deposition and molecular beam epitaxy growth. However, borophene has strong interaction with metallic substrates and poor stability under ambient conditions, and its transfer to an electrically insulating substrate remains elusive. Top-down approaches include mechanical and liquid exfoliation of bulk materials into 2D thin sheets. However, it is difficult to obtain 2D borophene with single atomic layer via these methods as the predominant structural unit of bulk boron is B_{12} icosahedra with 3D bonding. Moreover, obtaining neat boron nanosheets using this route is impossible due to the contamination by exfoliation agent and the instability of borop-

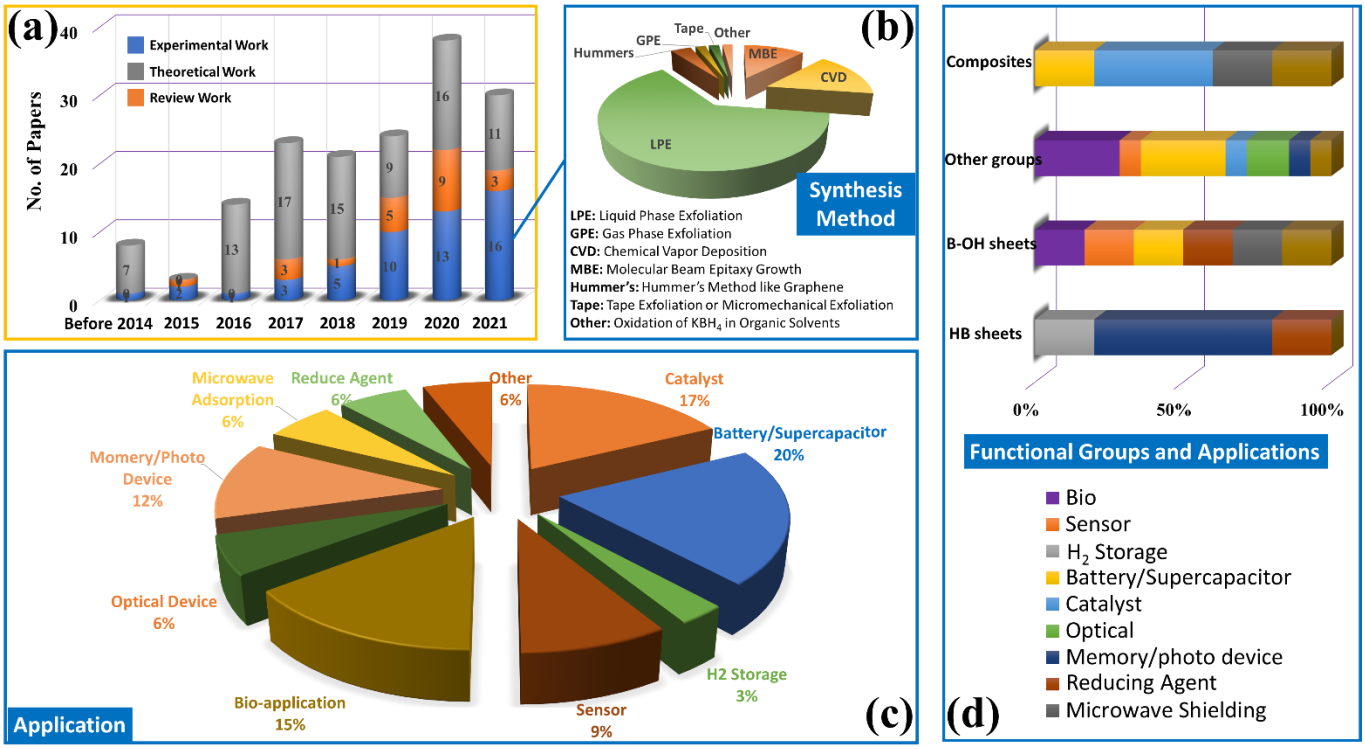

Figure 8. Recent publications on functionalized 2D boron. (a) Total number since 2015. (b) Breakdown of different methods used to obtain boron nanosheets. (c) Different applications tested in experiments. (d) Relation between tested applications and functional groups.

-hene. To summarize, despite the advances in theoretical studies, the synthesis of borophene is still at the incipient stage compared with well-studied 2D materials like graphene and TMDs.

Neat borophene or boron nanosheets has been theoretically predicted to show broad applications including photodevice [135, 136], electrocatalysis [137, 138], gas absorbing and sensing [139-142], anodes of batteries [143], and various drug or biomolecule sensing [144-146]. However, the ultra-high vacuum required for synthesis, poor stability and low throughput set back the applications of pristine borophene. To overcome the issue, various functional groups have been grafted to boron nanosheets. Furthermore, functionalization leads to new properties which render broader and practical applications.

Based on the literature cited in this review, a statistical analysis is conducted, and the results are displayed in **Figure 8**(a). Since the experimental synthesis of borophene was realized in 2015, publications related to 2D boron have been growing steadily. The number of experimental reports increases from 2 in 2015 to above 16 in 2021. LPE is the mostly applied method due to its low cost and ease of operation, featuring high yield and the simultaneous functionalization [Figure 8(b)]. The applications of functionalized boron nanosheets spans a broad range from bio-applications to catalysis, gas sensing, electronic devices, optics, and to batteries [Figure 8(c)]. In Figure 8(d), the applications of 2D boron are categorized according to functional groups, based upon which the following points are summarized.

(i) Chemical functional groups can be effectively introduced via the gaseous or liquid media used during fabrication. Functionalization by H atoms induces minimum impact on the metallic conductivity, making it suitable for electronic devices. HB has potential applications as a hydrogen carrier, a reducing agent, or a catalyst towards ethanol reforming. Oxygen functionalized boron nanosheets has been realized by oxidation in dry air. Oxygen functionalization leads to modified optical properties and potential applications in superconducting. The degree of oxidation affects the properties and applications. However, it is difficult to precisely control the degree of oxidation due to the strong electrophilicity of oxygen and the electron deficient nature of boron. Comparing with H and O, OH functionalization is much easier to be realized and can be controlled precisely. The B-OH nanosheets exhibit the properties of both -H and -O functionalized ones, such as modified optical property and the reducing capability. Moreover, the B-OH nanosheets is chemically stable and can maintain a high concentration dispersion in aqueous solution, paving the way for broader applications.

(ii) Elemental boron is electron deficient and can easily coordinate with nucleophilic functional groups such as carbonyl and alkyloxy groups, making the boron nanosheets chemically stable and suitable for various applications. Functional groups can tune properties by modifying the surface area, thickness, band gap, adsorption energy, dispersibility, and chemical reactivity.

(iii) Boron nanosheets doped by transition metals can be excellent gas sensors, gas carriers, and electrocatalysts, while nonmetal elements doped boron nanosheets have the potential of being used as high performance, light-weight anode materials in batteries, as suggested theoretically. So far, a precise control over heteroatom doping of borophene, especially at the atomic scale, has not been experimentally achieved.

(iv) Formation of composites featuring strong chemical interactions between boron nanosheets and the other component has attracted growing attentions. Firstly, boron nanosheets can be stabilized by these interactions, enabling wider applications. Second, an intriguing interface is generated, which brings about interesting properties to the composite. Lastly, the strong interaction can alter the properties of both components to certain degree. The application of these composites, therefore, could be significantly enhanced or broadened.

To summarize, compared with single-atomic-layered pristine borophene, functionalized 2D boron nanosheets possess promising applications in more diverse fields. Functional groups stabilize the structure and leads to new and versatile features, such as tuneable electronic structure, enhanced dispersibility, different sizes and surface areas, and variable adsorption energy towards different matters. All of these broaden the application prospect of 2D boron.

There are, however, challenges need to be overcome in relation to research on functionalized borophene. Hence, more efforts should be put into the following three directions. (i) The knowledge on the structure of borophene is still limited due to the complexity of boron chemistry, demonstrated by many different allotropes.[33, 34, 147-151] Therefore, more investigations on the allotropes of boropene are still needed. (ii) The synthesis of 2D boron nanosheets is still at the incipient stage in comparison with well-studied 2D materials like graphene and transition metal chalcogenides. Improved synthetic methods, especially the controllable and scalable ones, are needed to achieve structural precision at atomic scale and to realize the properties predicted theoretically. (iii) The current characterization of 2D boron is still somewhat 'murky' and oftentimes requires simulation to validate the experimental observation. Thus, it is important to identify and establish the characteristic signals unique to 2D boron nanosheets, i.e., spectral fingerprint, to allow rapid and accurate identification. For example, the current FTIR and XPS can not 100 % accurately distinguish the nature of the functional groups. Field-emission resonance spectroscopy within a scanning tunnelling microscope was recently used to reveal the local work function and interfacial charge transfer of borophene.[152] However, this technology is unsuitable for most functionalized boron nanosheets prepared via LPE due to various contaminants introduced during the fabrication.

Having said so, inspired by the sheer number of reports on the multi-field applications of graphene[153] and the recent exciting results on functionalized borophene and boron nanosheets, it is highly expected the research and applications on functionalized 2D boron will definitely soar in near future, and in both breadth and depth.

Conflicts of interest

There are no conflicts to declare.

Acknowledgements

Z. Huang acknowledges support under the Australian Research Council's Future Fellowship (FT190100658). W. Li is grateful for the support from a Discovery Early Career Researcher Award via DE180101478.

1 X. Chia and M. Pumera, *Nat. Catal.*, 2018, **1**, 909-921.
2 K. Khan, A. K. Tareen, M. Aslam, R. U. R. Sagar, B. Zhang, W. Huang, A. Mahmood, N. Mahmood, K. Khan, H. Zhang and Z. Guo, *Nano-Micro Lett.*, 2020, **12**, 167.
3 Y. Sun, S. Gao, F. Lei and Y. Xie, *Chem. Soc. Rev.*, 2015, **44**, 623-636.
4 C. Han, X. Wang, J. Peng, Q. Xia, S. Chou, G. Cheng, Z. Huang and W. Li, *Polymers*, 2021, **13**, 2137.
5 Z. Huang, S. Wang, R. D. Dewhurst, N. V. Ignat'ev, M. Finze and H. Braunschweig, *Angew. Chem. Intl. Ed.*, 2020, **59**, 8800-8816.
6 F. Liu, A. Nattestad, S. Naficy, R. Han, G. Casillas, A. Angeloski, X. Sun and Z. Huang, *Adv. Optical Mater.*, 2019, **7**, 1901380.
7 R. Han, F. Liu, X. Wang, M. Huang, W. Li, Y. Yamauchi, X. Sun and Z. Huang, *J. Mater. Chem. A*, 2020, **8**, 14384-14399.
8 M. H. Khan, H. K. Liu, X. Sun, Y. Yamauchi, Y. Bando, D. Golberg and Z. Huang, *Mater. Today*, 2017, **20**, 611-628.
9 R. Han, J. Diao, S. Kumar, A. Lyalin, T. Taketsugu, G. Casillas, C. Richardson, F. Liu, C. W. Yoon, H. Liu, X. Sun and Z. Huang, *J. Energy Chem.*, 2021, **57**, 477-484.
10 H. Chand, A. Kumar and V. Krishnan, *Adv. Mater. Interfaces*, 2021, **8**, 2100045.
11 C. Hou, G. Tai, Z. Wu and J. Hao, *ChemPlusChem*, 2020, **85**, 2186-2196.
12 K. Khan, A. K. Tareen, M. Aslam, M. F. Khan, Z. Shi, C. Ma, S. S. Shams, R. Khatoon, N. mahmood, H. Zhang and Z. Guo, *Prog. Solid State Chem.*, 2020, **59**, 100283.
13 D. Li, J. Gao, P. Cheng, J. He, Y. Yin, Y. Hu, L. Chen, Y. Cheng and J. Zhao, *Adv. Functn. Mater.*, 2020, **30**, 1904349.
14 X.-B. Li, S.-Y. Xie, H. Zheng, W. Q. Tian and H.-B. Sun, *Nanoscale*, 2015, **7**, 18863-18871.
15 M. Ou, X. Wang, L. Yu, C. Liu, W. Tao, X. Ji and L. Mei, *Adv. Sci.*, 2021, **8**, 2001801.
16 P. Ranjan, J. M. Lee, P. Kumar and A. Vinu, *Adv. Mater.*, 2020, **32**, 2000531.
17 P. Ranjan, T. K. Sahu, R. Bhushan, S. S. Yamijala, D. J. Late, P. Kumar and A. Vinu, *Adv. Mater.*, 2019, **31**, 1900353.
18 A. Rubab, N. Baig, M. Sher and M. Sohail, *Chem. Engin. J.*, 2020, **401**, 126109.
19 X. Sun, X. Liu, J. Yin, J. Yu, Y. Li, Y. Hang, X. Zhou, M. Yu, J. Li, G. Tai and W. Guo, *Adv. Functn. Mater.*, 2017, **27**, 1603300.
20 Z.-Q. Wang, T.-Y. Lü, H.-Q. Wang, Y. P. Feng and J.-C. Zheng, *Front. Phys.*, 2019, **14**, 33403.
21 X. Zhang, T. Wu, H. Wang, R. Zhao, H. Chen, T. Wang, P. Wei, Y. Luo, Y. Zhang and X. Sun, *ACS Catal.*, 2019, **9**, 4609-4615.
22 Z. Zhang, E. S. Penev and B. I. Yakobson, *Chem. Soc. Rev.*, 2017, **46**, 6746-6763.
23 P. Xiang, X. Chen, W. Zhang, J. Li, B. Xiao, L. Li and K. Deng, *Phys. Chem. Chem. Phys.*, 2017, **19**, 24945-24954.
24 B. Feng, J. Zhang, Q. Zhong, W. Li, S. Li, H. Li, P. Cheng, S. Meng, L. Chen and K. Wu, *Nat. Chem.*, 2016, **8**, 563-568.
25 W. Li, L. Kong, C. Chen, J. Gou, S. Sheng, W. Zhang, H. Li, L. Chen, P. Cheng and K. Wu, *Sci. Bull.*, 2018, **63**, 282-286.

26 A. J. Mannix, X.-F. Zhou, B. Kiraly, J. D. Wood, D. Alducin, B. D. Myers, X. Liu, B. L. Fisher, U. Santiago, J. R. Guest, M. J. Yacaman, A. Ponce, A. R. Oganov, M. C. Hersam and N. P. Guisinger, *Science*, 2015, **350**, 1513-1516.

27 X. Liu, Q. Li, Q. Ruan, M. S. Rahn, B. I. Yakobson and M. C. Hersam, *Nat. Mater.*, 2021, DOI: 10.1038/s41563-021-01084-2.

28 Y. Duo, Z. Xie, L. Wang, N. Mahmood Abbasi, T. Yang, Z. Li, G. Hu and H. Zhang, *Coord. Chem. Rev.,* 2021, **427**, 213549.

29 Z.-H. Cui, E. Jimenez-Izal and A. N. Alexandrova, *J. Phys. Chem, Lett.*, 2017, **8**, 1224-1228.

30 H. Gan, T. Zhang, Z. Guo, H. Lin, Z. Li, H. Chen, J. Chen and F. Liu, *Appl. Sci.*, 2019, **9**, 1019.

31 J. Hao, G. Tai, J. Zhou, R. Wang, C. Hou and W. Guo, *ACS Appl. Mater. Interfaces*, 2020, **12**, 17669-17675.

32 F. Liu, J. Tian, L. Bao, T. Yang, C. Shen, X. Lai, Z. Xiao, W. Xie, S. Deng, J. Chen, J. She, N. Xu and H. Gao, *Adv. Mater.*, 2008, **20**, 2609-2615.

33 X. Wu, J. Dai, Y. Zhao, Z. Zhuo, J. Yang and X. C. Zeng, *ACS Nano*, 2012, **6**, 7443-7453.

34 X.-F. Zhou, X. Dong, A. R. Oganov, Q. Zhu, Y. Tian and H.-T. Wang, *Phys. Rev. Lett.*, 2014, **112**, 085502.

35 C. Liu, Z. Dai, J. Zhang, Y. Jin, D. Li and C. Sun, *J. Phys. Chem. C*, 2018, **122**, 19051-19055.

36 D. Ma, J. Zhao, J. Xie, F. Zhang, R. Wang, L. Wu, W. Liang, D. Li, Y. Ge, J. Li, Y. Zhang and H. Zhang, *Nanoscale Horiz.*, 2020, **5**, 705-713.

37 X. Wang, J. Liang, Q. You, J. Zhu, F. Fang, Y. Xiang and J. Song, *Angew. Chem. Intl. Ed.*, 2020, **59**, 23559-23563.

38 C. Ma, P. Yin, K. Khan, A. K. Tareen, R. Huang, J. Du, Y. Zhang, Z. Shi, R. Cao, S. Wei, X. Wang, Y. Ge, Y. Song and L. Gao, *Small*, 2021, **17**, 2006891.

39 A. Joshi, A. K. Tomar, G. Singh and R. K. Sharma, *Chem. Engin. J.*, 2021, **407**, 127122.

40 M. Tatullo, B. Zavan, F. Genovese, B. Codispoti, I. Makeeva, S. Rengo, L. Fortunato and G. Spagnuolo, *Appl. Sci.*, 2019, **9**, 3446.

41 S.-Y. Xie, Y. Wang and X.-B. Li, *Adv. Mater.*, 2019, **31**, 1900392.

42 Z. Xie, X. Meng, X. Li, W. Liang, W. Huang, K. Chen, J. Chen, C. Xing, M. Qiu, B. Zhang, G. Nie, N. Xie, X. Yan and H. Zhang, *Research*, 2020, **2020**, 2624617.

43 H. Gunda, S. K. Das and K. Jasuja, *ChemPhysChem*, 2018, **19**, 880-891.

44 C. Hou, G. Tai, J. Hao, L. Sheng, B. Liu and Z. Wu, *Angew. Chem. Intl. Ed.*, 2020, **59**, 10819-10825.

45 Z. Fu, G. R. Williams, S. Niu, J. Wu, F. Gao, X. Zhang, Y. Yang, Y. Li and L.-M. Zhu, *Nanoscale*, 2020, **12**, 14739-14750.

46 A. L. Pickering, C. Mitterbauer, N. D. Browning, S. M. Kauzlarich and P. P. Power, *Chem. Commun.*, 2007, **6**, 580-582.

47 J. Xu, Y. Chang, L. Gan, Y. Ma and T. Zhai, *Adv. Sci.*, 2015, **2**, 1500023.

48 Z. Wu, G. Tai, R. Liu, C. Hou, W. Shao, X. Liang and Z. Wu, *ACS Appl. Mater. Interfaces*, 2021, **13**, 31808-31815.

49 H. Nishino, T. Fujita, N. T. Cuong, S. Tominaka, M. Miyauchi, S. Iimura, A. Hirata, N. Umezawa, S. Okada, E. Nishibori, A. Fujino, T. Fujimori, S.-i. Ito, J. Nakamura, H. Hosono and T. Kondo, *J. Am. Chem. Soc.*, 2017, **139**, 13761-13769.

50 R. Kawamura, N. T. Cuong, T. Fujita, R. Ishibiki, T. Hirabayashi, A. Yamaguchi, I. Matsuda, S. Okada, T. Kondo and M. Miyauchi, *Nat. Commun.*, 2019, **10**, 4880.

51 A. Fujino, S.-i. Ito, T. Goto, R. Ishibiki, J. N. Kondo, T. Fujitani, J. Nakamura, H. Hosono and T. Kondo, *ACS Omega*, 2019, **4**, 14100-14104.

52 Q. Li, V. S. C. Kolluru, M. S. Rahn, E. Schwenker, S. Li, R. G. Hennig, P. Darancet, M. K. Y. Chan and M. C. Hersam, *Science*, 2021, **371**, 1143-1148.

53 Y. Jiao, F. Ma, J. Bell, A. Bilic and A. Du, *Angew. Chem. Intl. Ed.*, 2016, **55**, 10292-10295.

54 K. I. M. Rojas, N. T. Cuong, H. Nishino, R. Ishibiki, S.-i. Ito, M. Miyauchi, Y. Fujimoto, S. Tominaka, S. Okada, H. Hosono, N. B. Arboleda, T. Kondo, Y. Morikawa and I. Hamada, *Commun. Mater.*, 2021, **2**, 81.

55 L.-C. Xu, A. Du and L. Kou, *Phys. Chem. Chem. Phys.*, 2016, **18**, 27284-27289.

56 N. Honari, S. M. Tabatabaei, M. Pourfath and M. Fathipour, *J. Phys. Chem. C*, 2020, **124**, 5807-5816.

57 Z. Wang, T.-Y. Lü, H.-Q. Wang, Y. P. Feng and J.-C. Zheng, *Phys. Chem. Chem. Phys.*, 2016, **18**, 31424-31430.

58 T. T. Xu, J.-G. Zheng, Wu, A. W. Nicholls, J. R. Roth, D. A. Dikin and R. S. Ruoff, *Nano Lett.*, 2004, **4**, 963-968.

59 Z. Wu, G. Tai, W. Shao, R. Wang and C. Hou, *Nanoscale*, 2020, **12**, 3787-3794.

60 S. Tominaka, R. Ishibiki, A. Fujino, K. Kawakami, K. Ohara, T. Masuda, I. Matsuda, H. Hosono and T. Kondo, *Chem*, 2020, **6**, 406-418.

61 A. Fujino, S.-i. Ito, T. Goto, R. Ishibiki, R. Osuga, J. N. Kondo, T. Fujitani, J. Nakamura, H. Hosono and T. Kondo, *Phys. Chem. Chem. Phys.*, 2021, **23**, 7724-7734.

62 X. Li, X. Tan, Q. Xue and S. Smith, *Int. J. Hydrogen Energy*, 2019, **44**, 20150-20157.

63 S.-i. Ito, T. Hirabayashi, R. Ishibiki, R. Kawamura, T. Goto, T. Fujita, A. Yamaguchi, H. Hosono, M. Miyauchi and T. Kondo, *Chem. Lett.*, 2020, **49**, 789-793.

64 P. Xiang, X. Chen, B. Xiao and Z. M. Wang, *ACS Appl. Mater. Interfaces*, 2019, **11**, 8115-8125.

65 A. Lherbier, A. R. Botello-Méndez and J.-C. Charlier, *2D Mater.*, 2016, **3**, 045006.

66 Y. He, N. Cheng, C. Chen, S. Xiong and J. Zhao, *Sci. China Technol. Sci.,* 2019, **62**, 799-810.

67 A. A. Kistanov, S. K. Khadiullin, S. V. Dmitriev and E. A. Korznikova, *Chem. Phys. Lett.*, 2019, **728**, 53-56.

68 J. C. Alvarez-Quiceno, R. H. Miwa, G. M. Dalpian and A. Fazzio, *2D Mater.*, 2017, **4**, 025025.

69 C. Zhong, W. Wu, J. He, G. Ding, Y. Liu, D. Li, S. A. Yang and G. Zhang, *Nanoscale*, 2019, **11**, 2468-2475.

70 L. Yan, P.-F. Liu, H. Li, Y. Tang, J. He, X. Huang, B.-T. Wang and L. Zhou, *NPJ Comput. Mater.*, 2020, **6**, 94.

71 T. Kambe, R. Hosono, S. Imaoka, A. Kuzume and K. Yamamoto, *J. Am. Chem. Soc.*, 2019, **141**, 12984-12988.

72 S. Chahal, P. Ranjan, M. Motlag, S. S. R. K. C. Yamijala, D. J. Late, E. H. S. Sadki, G. J. Cheng and P. Kumar, *Adv. Mater.*, 2021, **33**, 2102039.

73 D. P. Strommen and K. Nakamoto, *J. Chem. Education*, 1977, **54**, 474.

74 P. Habibi, T. J. H. Vlugt, P. Dey and O. A. Moultos, *ACS Appl. Mater. Interfaces*, 2021, **13**, 43233-43240.

75 R.-Y. Guo, T. Li, S.-E. Shi and T.-H. Li, *Mater. Chem. Phys.*, 2017, **198**, 346-353.

76 X. Ji, N. Kong, J. Wang, W. Li, Y. Xiao, S. T. Gan, Y. Zhang, Y. Li, X. Song, Q. Xiong, S. Shi, Z. Li, W. Tao, H. Zhang, L. Mei and J. Shi, *Adv. Mater.*, 2018, **30**, 1803031.

77 Q. Weng, X. Wang, X. Wang, Y. Bando and D. Golberg, *Chem. Soc. Rev.*, 2016, **45**, 3989-4012.

78 A. L. James and K. Jasuja, *RSC Advances*, 2017, **7**, 1905-1914.

79 A. L. James, S. Khandelwal, A. Dutta and K. Jasuja, *Nanoscale*, 2018, **10**, 20514-20518.

80 H. Nishino, T. Fujita, A. Yamamoto, T. Fujimori, A. Fujino, S.-i. Ito, J. Nakamura, H. Hosono and T. Kondo, *J. Phys. Chem. C*, 2017, **121**, 10587-10593.

81 R. Saraswat, A. L. James and K. Jasuja, *Adv. Appl. Ceramics*, 2019, **118**, 209-216.

82 P. Rohani, S. Kim and M. T. Swihart, *Adv. Energy Mater.*, 2016, **6**, 1502550.

83 Z. Zhang, M. Zhou, T. Zhang, M. Yang, Q. Yang, J. Yu and Y. Zhang, *ACS Appl. Mater. Interfaces*, 2020, **12**, 19746-19754.

84 M. S. Gilliam, A. Yousaf, Y. Guo, D. O. Li, A. Momenah, Q. H. Wang and A. A. Green, *Langmuir*, 2021, **37**, 1194-1205.
85 H. Li, L. Jing, W. Liu, J. Lin, R. Y. Tay, S. H. Tsang and E. H. T. Teo, *ACS Nano*, 2018, **12**, 1262-1272.
86 Q. Fan, C. Choi, C. Yan, Y. Liu, J. Qiu, S. Hong, Y. Jung and Z. Sun, *Chem. Commun.*, 2019, **55**, 4246-4249.
87 Q. Guo, K. Wu, Z. Shao, E. T. Basore, P. Jiang and J. Qiu, *Adv. Optical Mater.*, 2019, **7**, 1900322.
88 P. Qi, Q. Chen, D. Tu, S. Yao, Y. Zhang, J. Wang, C. Xie, C. Pan and H. Peng, *Biomater. Sci.*, 2020, **8**, 2778-2785.
89 Q. Zhou, H. Zhan, B. Chen, H. Li, Z. Huang, Y. Ma, H. Zhang, S. Li, X. Huang and W. Huang, *ACS Appl. Mater. Interfaces*, 2020, **12**, 23370-23377.
90 Y. Tao, Q. Wang, S. Ji, Y. Wang, Q. Zhou, Z. Huang, H. Li, X. Huang, B. Chen and S. Li, *Chem. Commun.*, 2021, **57**, 4922-4925.
91 H. Lin, H. Shi, Z. Wang, Y.-W. Mu, S.-D. Li, J. Zhao, J. Guo, B. Yang, Z.-S. Wu and F. Liu, *ACS Nano,* 2021, https://doi.org/10.1021/acsnano.1c04961.
92 C. Han, W. Li, H.-K. Liu, S. Dou and J. Wang, *Mater. Horiz.*, 2019, **6**, 1812-1827.
93 W. Li, C. Han, K. Zhang, S. Chou and S. Dou, *J. Mater. Chem. A*, 2021, **9**, 6671-6693.
94 J. K. Nørskov, F. Abild-Pedersen, F. Studt and T. Bligaard, *Proceed. Natl. Acad. Sci. U. S. A.*, 2011, **108**, 937-943.
95 M. Xu, X. Zhang, Y. Liu, X. Zhao, Y. Liu, R. Wu and J. Wang, *ChemPhysChem*, 2020, **21**, 2651-2659.
96 A. Banerjee, S. Chakraborty, N. K. Jena and R. Ahuja, *ACS Appl. Energy Mater.*, 2018, **1**, 3571-3576.
97 P. Zhang, X. Xu, E. Song, X. Hou, X. Yang, J. Mi, J. Huang and C. Stampfl, *Catal. Commun.*, 2020, **144**, 106090.
98 S. H. Mir, S. Chakraborty, P. C. Jha, J. Wärnå, H. Soni, P. K. Jha and R. Ahuja, *Appl. Phys. Lett.*, 2016, **109**, 053903.
99 Y. Singh, S. Back and Y. Jung, *Phys. Chem. Chem. Phys.*, 2018, **20**, 21095-21104.
100 X. Xu, R. Si, Y. Dong, L. Li, M. Zhang, X. Wu, J. Zhang, K. Fu, Y. Guo and Y. He, *J. Mol. Model.*, 2021, **27**, 67.
101 L. Xu, L.-M. Yang and E. Ganz, *ACS Appl. Mater. Interfaces*, 2021, **13**, 14091-14101.
102 X. Xu, X. Hou, J. Lu, P. Zhang, B. Xiao and J. Mi, *J. Phys. Chem. C*, 2020, **124**, 24156-24163.
103 S. Haldar, S. Mukherjee and C. V. Singh, *RSC Advances*, 2018, **8**, 20748-20757.
104 X. Kang, Z. Chu and X. Duan, *Appl. Surface Sci.*, 2021, **560**, 149667.
105 C. Liu, Q. Li, C. Wu, J. Zhang, Y. Jin, D. R. MacFarlane and C. Sun, *J. Am. Chem. Soc.*, 2019, **141**, 2884-2888.
106 Q. Xu, J. Zhang, H. Zhang, L. Zhang, L. Chen, Y. Hu, H. Jiang and C. Li, *Energy Environ. Sci.*, 2021, **14**, 5228-5259.
107 Q. Xu, H. Jiang, X. Duan, Z. Jiang, Y. Hu, S. W. Boettcher, W. Zhang, S. Guo and C. Li, *Nano Lett.*, 2021, **21**, 492-499.
108 H. Zhang, J. Wang, Q. Cheng, P. Saha and H. Jiang, *Green Energy Environ.*, 2020, **5**, 492-498.
109 V. Arefi, A. Horri and M. B. Tavakoli, *Comput. Theor. Chem.,* 2021, **1197**, 113159.
110 S. Kumar, M. Singh, D. K. Sharma and S. Auluck, *Comput. Condensed Matter*, 2020, **22**, e00436.
111 X. Chen, L. Wang, W. Zhang, J. Zhang and Y. Yuan, *Int. J. Hydrogen Energy*, 2017, **42**, 20036-20045.
112 L. Li, H. Zhang and X. Cheng, *Comput. Mater. Sci.*, 2017, **137**, 119-124.
113 L. Wang, X. Chen, H. Du, Y. Yuan, H. Qu and M. Zou, *Appl. Surface Sci.*, 2018, **427**, 1030-1037.
114 T. Z. Wen, A. Z. Xie, J. L. Li and Y. H. Yang, *Int. J. Hydrogen Energy*, 2020, **45**, 29059-29069.
115 X. Li, X. Li and J. Yang, *J. Phys. Chem, Lett.*, 2019, **10**, 4417-4421.
116 J. Y. Li, H. Y. Lv, W. J. Lu, D. F. Shao, R. C. Xiao and Y. P. Sun, *Phys. Lett. A*, 2016, **380**, 3928-3931.
117 C. Zhang, Z. Zhang, W. Yan and X. Qin, *Adv. Condensed Matter Phys.*, 2021, **2021**, 3718040.
118 F. Zergani and Z. Tavangar, *J. Mol. Liquids*, 2020, **319**, 114343.
119 H. Chen, W. Zhang, X.-Q. Tang, Y.-H. Ding, J.-R. Yin, Y. Jiang, P. Zhang and H. Jin, *Appl. Surface Sci.*, 2018, **427**, 198-205.
120 J. Khanifaev, R. Peköz, M. Konuk and E. Durgun, *Phys. Chem. Chem. Phys.*, 2017, **19**, 28963-28969.
121 X. Tang, J. Gu, J. Shang, Z. Chen and L. Kou, *InfoMat*, 2021, **3**, 327-336.
122 I. Muhammad, U. Younis, H. Xie, A. A. Khan, A. Khaliq, A. Samad, U. Schwingenschlögl and Q. Sun, *Chem. Mater.*, 2021, **33**, 2976-2983.
123 W. Shao, G. Tai, C. Hou, Z. Wu, Z. Wu and X. Liang, *ACS Appl. Electronic Mater.*, 2021, **3**, 1133-1141.
124 K. Chen, Z. Wang, L. Wang, X. Wu, B. Hu, Z. Liu and M. Wu, *Nano-Micro Lett.*, 2021, **13**, 138.
125 C. Taşaltın, T. A. Türkmen, N. Taşaltın and S. Karakuş, *J. Mater. Sci: Mater. Electronics*, 2021, **32**, 10750-10760.
126 S. Wang, Q. Li, K. Hu, Q. Liu, X. Liu and X. Kong, *Compos. Part A Appl. Sci. Manuf.*, 2020, **138**, 106033.
127 C. Hou, G. a. Tai, B. Liu, Z. Wu and Y. Yin, *Nano Res.*, 2021, **14**, 2337-2344.
128 C. Long, X. Xie, J. Fu, Q. Wang, H. Guo, W. Zeng, N. Wei, S. Wang and Y. Xiong, *J. Colloid Interface Sci.*, 2021, **601**, 355-364.
126 T. Wu, X. Wu, L. Li, M. Hao, G. Wu, T. Zhang and S. Chen, *Angew. Chem. Intl. Ed.*, 2020, **59**, 23800-23809.
129 J. Shen, Z. Yang, Y. Wang, L.-C. Xu, R. Liu and X. Liu, *Appl. Surface Sci.*, 2020, **504**, 144412.
131 C. Hou, G. Tai, Y. Liu, Z. Wu, Z. Wu and X. Liang, *J. Mater. Chem. A*, 2021, **9**, 13100-13108.
132 J. Yin, X. You, Z. Zhang, Z. Guo, J. Wang and X. Wang, *J. Water Process Engin.*, 2021, **41**, 102048.
133 H. Li, J. Hou, Q. Duan and D. Jiang, *Appl. Surface Sci.*, 2021, **545**, 148770.
134 Q. Li, J. Yang and L. Zhang, *J. Phys. Chem. C*, 2018, **122**, 18294-18303.
135 Y. Tian, Z. Guo, T. Zhang, H. Lin, Z. Li, J. Chen, S. Deng and F. Liu, *Nanomaterials*, 2019, **9**, 538.
136 L.-S. Wang, *Int. Rev. Phys. Chem.,* 2016, **35**, 69-142.
137 G. Qin, Q. Cui, A. Du and Q. Sun, *ChemCatChem*, 2020, **12**, 1483-1490.
138 F. J. Owens, *Chem. Phys. Lett.*, 2018, **691**, 131-134.
139 X. Tan, H. A. Tahini and S. C. Smith, *ACS Appl. Mater. Interfaces*, 2017, **9**, 19825-19830.
140 V. Shukla, J. Wärnå, N. K. Jena, A. Grigoriev and R. Ahuja, *J. Phys. Chem. C*, 2017, **121**, 26869-26876.
141 V. Nagarajan and R. Chandiramouli, *Comput. Theor. Chem.*, 2017, **1105**, 52-60.
142 C.-S. Huang, A. Murat, V. Babar, E. Montes and U. Schwingenschlögl, *J. Phys. Chem. C*, 2018, **122**, 14665-14670.
143 H. R. Jiang, Z. Lu, M. C. Wu, F. Ciucci and T. S. Zhao, *Nano Energy*, 2016, **23**, 97-104.
144 S. Sabokdast, A. Horri, Y. T. Azar, M. Momeni and M. b. Tavakoli, *Phys. E Low Dimens. Syst. Nanostruct.*, 2020, **119**, 114026.
145 A. Rastgou, H. Soleymanabadi and A. Bodaghi, *Microelectron. Engin.*, 2017, **169**, 9-15.
146 C. Xiao, K. Ma, G. Cai, X. Zhang and E. Vessally, *J. Mol. Graph. Model.* 2020, **96**, 107539.
147 E. S. Penev, S. Bhowmick, A. Sadrzadeh and B. I. Yakobson, *Nano Lett.*, 2012, **12**, 2441-2445.
148 W.-L. Li, Q. Chen, W.-J. Tian, H. Bai, Y.-F. Zhao, H.-S. Hu, J. Li, H.-J. Zhai, S.-D. Li and L.-S. Wang, *J. Am. Chem. Soc.*, 2014, **136**, 12257-12260.
149 Z. A. Piazza, H.-S. Hu, W.-L. Li, Y.-F. Zhao, J. Li and L.-S. Wang, *Nat. Commun.*, 2014, **5**, 3113.

150 M. G. Mohamed, E. C. Atayde, B. M. Matsagar, J. Na, Y. Yamauchi, K. C. W. Wu and S.-W. Kuo, *J. Taiwan Inst. Chem. Eng.*, 2020, **112**, 180-192.
151 M. M. Samy, M. G. Mohamed, A. F. M. El-Mahdy, T. H. Mansoure, K. C. W. Wu and S.-W. Kuo, *ACS Appl. Mater. Interfaces*, 2021, **13**, 51906-51916.
152 X. Liu, L. Wang, B. I. Yakobson and M. C. Hersam, *Nano Lett.*, 2021, **21**, 1169-1174.
153 P. P. Brisebois and M. Siaj, *J. Mater. Chem. C*, 2020, **8**, 1517-1547.